THE JOURNAL OF BIOLOGICAL CHEMISTRY
Vol. 279, No. 23, Issue of June 4, pp. 24803–24812, 2004
Printed in U.S.A.

Role of a Conserved Arginine in the Mechanism of Acetohydroxyacid Synthase

CATALYSIS OF CONDENSATION WITH A SPECIFIC KETOACID SUBSTRATE*

Received for publication, February 15, 2004, and in revised form, March 18, 2004
Published, JBC Papers in Press, March 25, 2004, DOI 10.1074/jbc.M401667200

Stanislav Engel‡§¶, Maria Vyazmensky¶‖, Michael Vinogradov‖, Dvora Berkovich‡, Ahuva Bar-Ilan‖, Udi Qimron‖**, Yogev Rosiansky‖, Ze'ev Barak‖, and David M. Chipman‖‡‡**

From the ‖Department of Life Sciences and ‡Department of Biotechnology Engineering, Ben-Gurion University of the Negev, POB 653, 84105 Beer-Sheva, Israel

The thiamin diphosphate (ThDP)-dependent biosynthetic enzyme acetohydroxyacid synthase (AHAS) catalyzes decarboxylation of pyruvate and specific condensation of the resulting ThDP-bound two-carbon intermediate, hydroxyethyl-ThDP anion/enamine (HEThDP$^-$), with a second ketoacid, to form acetolactate or acetohydroxybutyrate. Whereas the mechanism of formation of HEThDP$^-$ from pyruvate is well understood, the role of the enzyme in control of the carboligation reaction of HEThDP$^-$ is not. Recent crystal structures of yeast AHAS from Duggleby's laboratory suggested that an arginine residue might interact with the second ketoacid substrate. Mutagenesis of this completely conserved residue in *Escherichia coli* AHAS isozyme II (Arg^{276}) confirms that it is required for rapid and specific reaction of the second ketoacid. In the mutant proteins, the normally rapid second phase of the reaction becomes rate-determining. A competing alternative nonnatural but stereospecific reaction of bound HEThDP$^-$ with benzaldehyde to form phenylacetylcarbinol (Engel, S., Vyazmensky, M., Geresh, S., Barak, Z., and Chipman, D. M. (2003) *Biotechnol. Bioeng.* 84, 833–840) provides a new tool for studying the fate of HEThDP$^-$ in AHAS, since the formation of the new product has a very different dependence on active site modifications than does acetohydroxyacid acid formation. The effects of mutagenesis of four different residues in the site on the rates and specificities of the normal and unnatural reactions support a critical role for Arg^{276} in the stabilization of the transition states for ligation of the incoming second ketoacid with HEThDP$^-$ and/or for the breaking of the product-ThDP bond. This information makes it possible to engineer the active site so that it efficiently and preferentially catalyzes a new reaction.

Acetohydroxyacid synthase (AHAS)[1] belongs to a homologous family of thiamin diphosphate (ThDP)-dependent enzymes that catalyze reactions whose initial step is decarboxylation of pyruvate or another 2-ketoacid (1, 2). However, despite the similarity of AHASs to, for example, pyruvate decarboxylases and pyruvate oxidases (3–6), AHASs carry out a specific carboligation reaction in which the decarboxylation of pyruvate is followed by the condensation of the bound hydroxyethyl-ThDP anion/enamine (HEThDP$^-$) intermediate with a second aliphatic ketoacid to form an acetohydroxyacid (Fig. 1). Whereas the role of the enzyme in the first steps in AHAS catalysis (*i.e.* activation of ThDP (7), decarboxylation of pyruvate, and formation of HEThDP$^-$ (step 1 in Fig. 1)) is comparable with the function of other members of its homologous family (8), it has been difficult to suggest roles for specific protein residues in the final steps (2 and 3) of the reaction in which the product acetohydroxyacid is formed and released.

One reason for this uncertainty has been the lack of clear direct information on the structure of the regions of the active site that might be involved in selective reaction of HEThDP$^-$ with a second ketoacid. Although we have proposed a homology model for AHAS isozyme II from *Escherichia coli* (9), based on the crystal structure of pyruvate oxidase from *Lactobacillus plantarum* (LpPOX) (4), these two proteins have very different sequences in the region that is likely to interact with the second substrate. In the first published crystal structure of an AHAS, that of the catalytic subunits of the yeast enzyme (10), this region was disordered. The recent publication of a new structure of the yeast enzyme with a tightly bound herbicide (11) now provides a solid framework for consideration of the role of the protein in directing the fate of the HEThDP$^-$ intermediate.

A second, equally serious obstacle to the understanding of the mechanism of AHAS has been a lack of experimental tools for studying the rates of individual steps in the reaction and, thus, the effects of modifications of the enzyme on these steps. Ciskanik and Schloss (12) showed that HEThDP$^-$ does not accumulate significantly in the reaction of AHAS II, so that following the formation and disappearance of covalent intermediates in presteady state experiments would be difficult. We were able to use the competition between pyruvate and 2-ketobutyrate (13), the two physiological second substrates that can react with the intermediate on AHAS, to show that the formation of the common intermediate is rate-determining and

* This work was supported in part by Israel Science Foundation Grant 660/01 (to Z. B.), by a seed grant from the Vice President for Research and Development at Ben-Gurion University (to D. M. C.), and by a grant from the Fund for Applied Research, administered by BG Negev Technologies (to D. M. C. and Z. B.). The costs of publication of this article were defrayed in part by the payment of page charges. This article must therefore be hereby marked "*advertisement*" in accordance with 18 U.S.C. Section 1734 solely to indicate this fact.

§ A Kreitman Foundation Doctoral Fellow.

¶ These two authors contributed equally to this work.

** Current address: Dept. of Immunology and Microbiology, Faculty of Health Sciences, Ben-Gurion University of the Negev, POB 653, 84105 Beer-Sheva, Israel.

‡‡ Incumbent of the Lily and Sidney Oelbaum Chair in Applied Biochemistry at Ben-Gurion University. To whom correspondence should be addressed. Tel.: 972-8-647-2646; Fax: 972-8-646-1710; E-mail: chipman@bgumail.bgu.ac.il.

[1] The abbreviations used are: AHAS, acetohydroxyacid synthase; ThDP, thiamin diphosphate; HEThDP$^-$, hydroxyethyl-ThDP anion/enamine; KB, 2-ketobutyrate; AL, acetolactate; AHB, acetohydroxybutyrate; PAC, phenyl acetyl carbinol; CIE, chlorimuron ethyl; BA, benzaldehyde; HPLC, high pressure liquid chromatography; DTT, dithiothreitol.

that the step that determines *which* product will be formed probably comes after $HEThDP^-$ formation (14). The competition between second substrates was also used to identify a tryptophan residue critical for the high preference of most AHASs for 2-ketobutyrate (9). An interesting side reaction, leading to peracetate formation in AHAS II, showed that oxygen could compete with the natural substrates for the intermediate (15, 16), but this very slow reaction is not appropriate for study of the function of residues in the enzyme active site. Tittmann *et al.* (17) have recently developed a quenched proton magnetic resonance technique for determining the partition of ThDP among various covalent intermediates in an enzymic reaction. For AHAS II, Tittmann *et al.* (17) demonstrated that by far the slowest step is formation of the first covalent intermediate, lactyl-ThDP.

We have recently found that AHASs can catalyze an alternative reaction, in which an aromatic aldehyde reacts with the intermediate $HEThDP^-$ to form an arylacetylcarbinol (Fig. 1) with very high enantiomeric specificity (18). The stereochemistry, kinetics, and specificity of the competition between pyruvate and benzaldehyde shed light on the location of the reacting substrates in the active site of AHAS and can be used to identify residues in the enzyme that interact with the alternative electrophilic reagents. In particular, this approach has allowed us to identify Arg^{276} as crucial to the specificity of the enzyme for condensation with a second ketoacid.

EXPERIMENTAL PROCEDURES

Reagents—Hepes, sodium pyruvate, FAD, ThDP, dithiothreitol (DTT), ethyl 2-acetoxy-2-methyl acetoacetate, benzaldehyde, and Me_2SO were obtained from Sigma. Racemic acetolactate was prepared by basic (KOH) hydrolysis of ethyl 2-acetoxy-2-methyl-acetoacetate as previously described (19). The concentration of *S*-acetolactate after conversion was determined from the spectrophotometric assay of NADPH oxidation by ketolacid reductoisomerase (20), which is quite specific for the *S* configuration (21). All other materials were of analytical grade.

Construction of Plasmids pRSET-GM and pQEV-GM—XL-1-Blue MRF′ strain (Stratagene Europe) was used as the host strain in construction of wild-type and mutated plasmids. In the initial phase of our work, we used the plasmid pRSET-GM for expression of a hexahistidine-tagged AHAS II. This plasmid was obtained by inserting the BamHI-EcoRI fragment containing the *ilvGM* genes from pET-GM (a gift from R. G. Duggleby (22)) into plasmid pRSET A (Invitrogen). Most of the coding region was then replaced by inserting the NsiI-EcoRI fragment from pRGM (8) to create pRSET-GM, which expresses a protein with a sequence identical to the original AHAS II enzyme of *E. coli ilvG*2096 fused at its N terminus to the pRSET hexahistidine leader. pRSET-GM was transformed into BL21(DE3) for expression.

In later work, the identical protein was expressed from plasmid pQEV-GM, a derivative of expression plasmid pQE60 (Qiagen, Hilden, Germany) for which *E. coli* XL-MRF serves as host, in a system that we found to be more stable and easier to work with. A unique NdeI site was constructed immediately downstream of the promoter of pQE60, and the original unique NdeI site (bp 1370 from ORI) was destroyed using the QuikChange™ site-directed mutagenesis kit (Stratagene, La Jolla, CA) to create plasmid pQE601.[2] Two separate fragments from pRSET-GM (the first a 975-bp NdeI-NdeI fragment that includes the polyhistidine region and 5′-end of *ilvG* and the second a 1039-bp NdeI-HindIII fragment that includes the remainder of *ilvGM*) were then ligated into the NdeI-HindIII sites of the pQE601 polylinker.

Mutagenesis—Mutations were introduced in pQEV-GM at positions corresponding to residues Phe^{109} and Arg^{276} using the QuikChange™ site-directed mutagenesis kit (Stratagene, La Jolla, CA). The primers used were designed to introduce an additional restriction site or destroy existing sites, as an aid in screening for clones with mutated plasmids. Mutations were introduced at residues Trp^{464} (9) and Met^{250} using the PCR overlap extension method (23). Fragments containing the mutation were excised from the original mutated plasmids and introduced by ligation into pQEV-GM. The complete coding region of each plasmid used for mutein expression was sequenced.

[2] H. Shmueli, personal communication.

Preparation of Enzymes—Bacterial growth and expression of cloned genes were carried out as described elsewhere (8). Wild-type AHAS isozyme II from *E. coli* and all of the mutated variants (muteins) of AHAS II whose properties are described here were obtained as N-terminal hexahistidine-tagged proteins overexpressed in XL-1-Blue MRF′. Bacterial cells were disrupted by sonication in a buffer (buffer A) with 10 mM imidazole, 0.5 M KCl, 50 mM Tris-HCl, pH 8.0, and 20 μM FAD. After 1 h of centrifugation at 27,000 × *g*, the supernatant was loaded on a 1 × 5.5-cm column of Ni^{2+}-nitrilotriacetic acid-agarose (Qiagen, Hilden, Germany) previously washed with buffer A. The column was then washed with ~50 ml of buffer A (until no more protein eluted), and the His′-GM protein eluted with a buffer identical to A except for the addition of 0.4 M imidazole. The fractions were dialyzed against 50 mM KP_i, pH 7.6, containing 20 μM FAD and 1 mM DTT.

The protein was concentrated for storage at −20 °C by dialysis against 50 mM KP_i, pH 7.6, containing 1 mM DTT, 20 μM FAD, 10% polyethylene glycol 20000 (Merck Schuchart, Darmstadt) and 50% glycerol.

Enzyme assays were carried out using the methods previously described (8) in a 0.1 M potassium phosphate buffer (pH 7.6) containing 10 mM $MgCl_2$, 0.1 mM ThDP, and 75 μM FAD, with 100 mM pyruvate as substrate, except where otherwise indicated.

The ketoacid substrate competition experiments were carried out in the same buffer, by measuring acetohydroxybutyrate and acetolactate formation simultaneously in reaction mixtures containing 2-ketobutyrate and pyruvate (14), and analyzed by fitting the data to appropriate equations using the nonlinear least squares program SigmaPlot 2000 (SPSS, Inc.). At a given constant pyruvate concentration, the total rate of acetohydroxyacid production by wild type and some mutants of AHAS II, *V*, is constant (9, 14), and the 2-ketobutyrate dependence of the individual rates (V_{AL} and V_{AHB}) can be fit simultaneously to Equations 1 and 2.

$$V_{AL} = V\cdot[Pyr] / ([Pyr] + R\cdot[KB]) \quad \text{(Eq. 1)}$$

$$V_{AHB} = V\cdot R\cdot[KB] / ([Pyr] + R\cdot[KB]) \quad \text{(Eq. 2)}$$

R is the characteristic 2-ketobutyrate specificity parameter for a given enzyme, defined by $R = (V_{AHB}/V_{AL})\cdot([Pyr]/[KB])$. For muteins where the total rate is not constant, Equations 3 and 4 hold as follows,

$$V_{AL} = V_a\cdot[Pyr] / ([Pyr] + f\cdot[KB]) \quad \text{(Eq. 3)}$$

$$V_{AHB} = V_b\cdot f\cdot[KB] / ([Pyr] + f\cdot[KB]) \quad \text{(Eq. 4)}$$

where V_a is the rate in the absence of 2-ketobutyrate, V_b is the rate of acetohydroxybutyrate formation at saturation with 2-ketobutyrate, and *f* is a characteristic parameter for the enzyme. If Equations 3 and 4 hold, then the characteristic specificity of the enzyme is given by $R = f\cdot V_b/V_a$.

Reactions with benzaldehyde were carried out at 30 °C, in the presence of 0.1 M Hepes/KOH, pH 7.0, 5 mM $MgCl_2$, 0.1 mM ThDP, 0.05 mM FAD, 60 mM KCl, 0.5 mM DTT, and varied amounts of pyruvate and benzaldehyde. The reaction mixture contained Me_2SO to facilitate dissolution of benzaldehyde. Reactions were initiated by the addition of enzyme.

Analyses—For HPLC analyses of phenyl acetyl carbinol (PAC) formation, the enzymatic reaction was terminated by heating at 100 °C for 2 min, and the precipitated protein was removed by centrifugation. The HPLC separations were carried out as previously described on a C18-TSKgel ODS-80TM 5 μm column (250 × 4.6 mm) (TosoHaas) with 30% acetonitrile, 0.5% acetic acid (v/v) as eluent (18).

A creatine-naphthol colorimetric method was used for the simultaneous assay of acetolactate and PAC (18). In this method, the colored products derived from PAC and acetolactate have different absorbance spectra, allowing the calculation of the concentrations of both products from absorbance at two wavelengths with simultaneous equations (18). Absorbance was measured with a Beckman DU640 spectrophotometer.

Circular dichroism was measured on a Jasco model J715 spectropolarimeter. We have found[3] that circular dichroism can be reliably used for following reactions of AHAS. At 310 nm, *S*-acetolactate has a molar ellipticity of +2460 degrees cm^2 $dmol^{-1}$, and *R*-PAC has a molar ellipticity of −2390 degrees cm^2 $dmol^{-1}$.

Protein concentration was measured by the method of Bradford, using bovine serum albumin as a standard.

[3] M. Vinogradov, A. Kaplun, M. Vyazmensky, R. Golbik, K. Uhlemann, L. Meshalkina, Z. Barak, G. Hübner, and D. M. Chipman, manuscript in preparation.

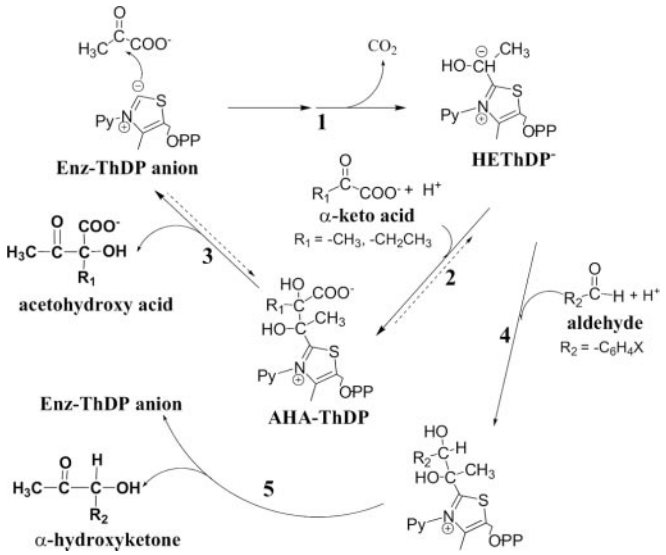

FIG. 1. **The reactions catalyzed by AHAS.** The bound ThDP anion reacts with pyruvate to form lactyl-ThDP, which undergoes decarboxylation to form hydroxyethylThDP (*step 1*). Either of two ketoacids, pyruvate or 2-ketobutyrate, reacts with the intermediate (*step 2*) to form a bound acetohydroxyacid (AHA-ThDP), which is then released (*step 3*). In the presence of an appropriate aryl aldehyde the $HEThDP^-$ intermediate can react with the aldehyde to form a bound arylacetyl carbinol (*step 4*), which is released (*step 5*) as a nonphysiological product.

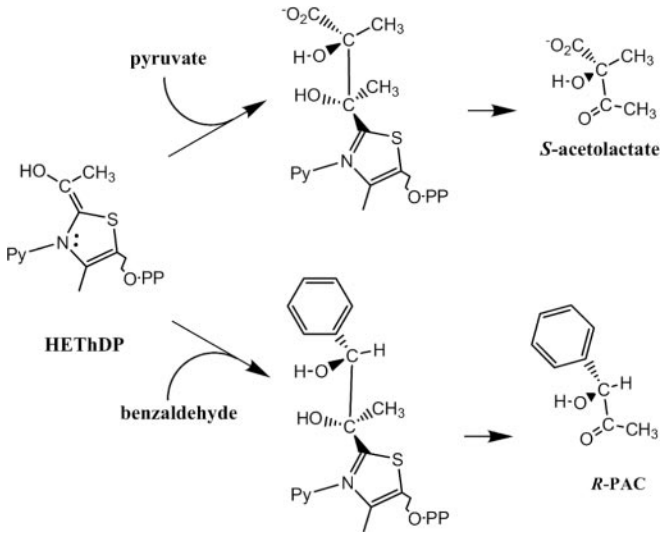

FIG. 2. **Stereochemical outcome of reactions with pyruvate or benzaldehyde as second substrate.** Note that, since the carbon bound to C-2 of the cofactor becomes trigonal when the product is released, its configuration in the ThDP-product compounds is not known from experiments. However, the configuration shown is reasonable on the basis of the enzyme structure and ThDP chemistry.

RESULTS

Kinetics of Synthesis of Phenyl Acetyl Carbinol—We have found that, in addition to catalyzing the physiological reactions leading to the formation of acetohydroxybutyrate and acetolactate (Fig. 1) (24), AHAS II can catalyze the formation of *R*-phenyl acetyl carbinol (*R*-PAC) from pyruvate and benzaldehyde (18). AHAS II specifically forms *R*-PAC with an enantiomeric excess of >98% (18), whereas the acetohydroxyacid products formed by AHAS have the *S* absolute configuration (25). If one assumes that the carbonyl groups of the alternative second substrates all make similar contacts in the enzyme active site as they react with $HEThDP^-$, then the aromatic ring of benzaldehyde and the carboxyl group of a ketoacid must occupy the same general region in the site. The hydrogen on the new chiral carbon of *R*-PAC would thus point in the same direction as the methyl (or ethyl) group of the acetohydroxyacid (Fig. 2). If this analysis is correct, then different residues in the enzyme active site must be involved in determining the preference for pyruvate, 2-ketobutyrate, or benzaldehyde as the second substrate. This prediction has been born out by a series of competition experiments with wild-type AHAS II and its variants.

In experiments where the concentration of pyruvate is held constant and that of 2-ketobutyrate is raised, the initial rate of formation of acetolactate (V_{AL}) is slowed, and that of acetohydroxybutyrate (V_{AHB}) is increased (9, 14) (Fig. 3*A*). The total rate of acetohydroxyacid formation by wild-type AHAS II remains essentially constant, and the rates can be fit simultaneously to Equations 1 and 2 (see "Experimental Procedures"). For this enzyme, *R*, the preference for reaction with ketobutyrate, is close to 60.

Acetolactate formation is also inhibited in the presence of benzaldehyde, and the initial rate of synthesis of acetolactate decreases and the rate of *R*-PAC synthesis increases as the concentration of benzaldehyde is raised (Fig. 3*B*). Equations 5 and 6 describing the dependence of the rates of formation of acetolactate and PAC (V_{PAC}) at a given pyruvate and varying benzaldehyde (BA) concentrations would be the equivalent of Equations 3 and 4.

$$V_{AL} = V_a \cdot [Pyr] / ([Pyr] + f[BA]) \quad \text{(Eq. 5)}$$

$$V_{PAC} = V_c f \cdot [BA] / ([Pyr] + f \cdot [BA]) \quad \text{(Eq. 6)}$$

In this case, however, the total rate of the two reactions decreases with increasing aldehyde, so that the overall influence of the benzaldehyde concentration on the rates of formation of acetolactate and PAC can only be fit by Equations 7 and 8, in which the rates are multiplied by an inhibition term, $K_i/(K_i + [BA])$,

$$V_{AL} = V_a \cdot K_i \cdot [Pyr] / (([Pyr] + f \cdot [BA])(K_i + [BA])) \quad \text{(Eq. 7)}$$

$$V_{PAC} = V_c \cdot K_i f \cdot [BA] / (([Pyr] + f \cdot [BA])(K_i + [BA])) \quad \text{(Eq. 8)}$$

where V_c is the rate at which PAC would be formed at saturating benzaldehyde if there were no overall inhibition, and K_i is an apparent inhibition constant for benzaldehyde. The apparent inhibition constant K_i is about 25 mM for wild-type enzyme.

Since we have not demonstrated the kinetic details of the competition between pyruvate and benzaldehyde and have not measured the dependence of the two rates over a range of benzaldehyde concentrations for all of the muteins described here, we define a measure of the preference of an enzyme for formation of *R*-PAC, $\tilde{R}_{Bz}$, as the ratio of the initial rates of formation of *R*-PAC and acetolactate when the two are measured simultaneously in the presence of 30 mM each of pyruvate and benzaldehyde. For the wild-type AHAS II, the rates of the two competing processes are approximately equal when concentrations of benzaldehyde and pyruvate are both 30 mM, with specific rates of formation of acetolactate and *R*-PAC of 2.9 and 3.3 μmol min^{-1} mg^{-1}, respectively. Thus, $\tilde{R}_{Bz}$ for wild-type AHAS II is 1.14 (Table I).

The limited solubility of benzaldehyde did not allow us to determine whether very high concentrations of benzaldehyde inhibit acetolactate formation completely. However, we could examine the competition between benzaldehyde and 2-ketobutyrate for the $HEThDP^-$ intermediate by following the rate of PAC formation in the presence of a constant concentration of both benzaldehyde and pyruvate, with increasing amounts of 2-ketobutyrate. The measurements of the rates of PAC formation are inaccurate at the lowest concentrations of 2-ketobutyrate; because of the high preference of the enzyme for

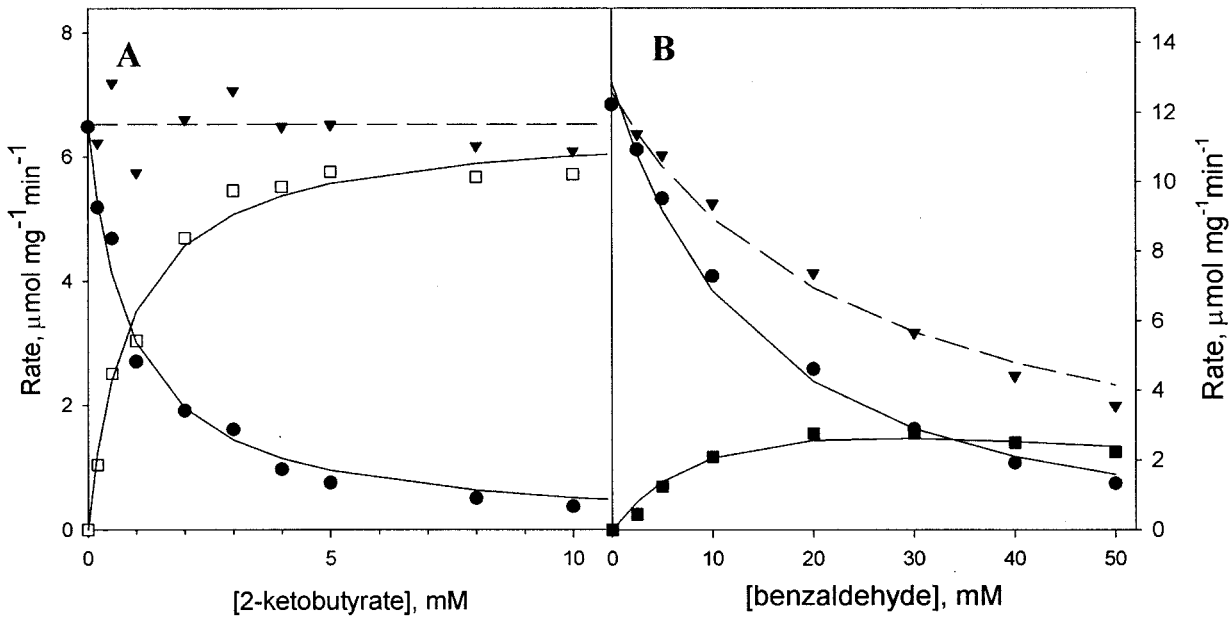

FIG. 3. *A*, effect of 2-ketobutyrate concentration on the initial rates of formation of acetohydroxybutyrate (□) and acetolactate (●) by wild-type AHAS II at 37 °C, in 0.1 M potassium phosphate buffer (pH 7.6) containing 10 mM $MgCl_2$, 0.1 mM ThDP, and 0.075 mM FAD, with 50 mM pyruvate as substrate and varied concentrations of 2-ketobutyrate. The amount of acetolactate and acetohydroxybutyrate formed after a 6-min reaction with 2.58 μg/ml of enzyme was measured as previously described (14). The sum of the rates of formation of the two acetohydroxyacids (▼) is also shown. *B*, effect of benzaldehyde on the initial rates of PAC (■) and acetolactate (●) formation by AHAS II. The reaction was carried out with 60 μg/ml AHAS II at 30 °C for 10 min, in 0.1 M Hepes/KOH buffer, pH 7.0, containing 5 mM $MgCl_2$, 0.1 mM ThDP, 0.05 mM FAD, 60 mM KCl and 10% (v/v) Me_2SO. Initial rates of formation of acetolactate and PAC were determined by the simultaneous colorimetric method, as described under "Experimental Procedures." The sum of the rates of formation of the two products (▼) is also shown. The results were fit simultaneously to Equations 7 and 8.

TABLE I
Properties of AHAS II and its mutants

AHAS II with an N-terminal hexahistidine fusion, as well as point mutants derived from it, was expressed from XL-1-Blue MRF′/pQEV-GM and purified on a nickel chelate column.

Enzyme	Spec. Act. (acetolactate)[a]	k_{cat}/K_m (pyruvate)	Ketobutyrate preference[b] (R_{KB})	Reaction with 30 mM pyruvate + 30 mM benzaldehyde[c]		
				AL formation Spec. Act.	PAC formation Spec. Act.	$\tilde{R}_{Bz}$[e]
	units mg^{-1}	M^{-1} s^{-1}				
Wild type	17	6600	59	2.9	3.3	1.14
F109L	0.81	56	40	0.03	0.54	18
F109M	1.7	140	63	ND[d]	4.28	∞
F109W	0.87	36	60	0.007	0.1	14.3
M250A	1.8	130	56	0.13	2.3	17.8
R276M	0.32	11	0.4	ND	0.96	∞
R276F	0.28	14	0.4	0.06	1.0	16.7
R276Q	0.2	8	0.9	0.017	0.59	35
R276K	2.8	170	28	0.19	4.1	21.6
W464L	11.9	2500	3.0	3.8	3.4	0.90
W464Q	9.3	690	4.0	2.5	2.1	0.84
W464A	6.1	691	4.0	1.8	1.7	0.91
W464Y	7.5	1750	9.1	5.4	2.3	0.43

[a] Specific activity (Spec. Act.) in the synthesis of acetolactate with 50 mM pyruvate as sole substrate was determined in 0.1 M potassium phosphate buffer (pH 7.6) containing 10 mM $MgCl_2$, 0.1 mM ThDP, and 0.075 mM FAD. One unit = 1 μmol of acetolactate min^{-1}.

[b] The specificity for the reaction with 2-ketobutyrate was measured as described under "Experimental Procedures" in the presence of 50 mM pyruvate and varying amounts of 2-ketobutyrate. $R_{KB} = (V_{AHB}/V_{AL})$ /([2KB]/[pyruvate]), where V_{AHB} and V_{AL} are the rates of formation of acetohydroxybutyrate and acetolactate, respectively.

[c] The formation of acetolactate and *R*-PAC was measured by the simultaneous colorimetric assay in 0.1 M Hepes/KOH, pH 7.0, 5 mM $MgCl_2$, 0.1 mM ThDP, 0.05 mM FAD, 60 mM KCl, 0.5 mM DTT, 10% Me_2SO_4 (v/v) in the presence of 30 mM each of pyruvate and benzaldehyde. Specific activities are in units of μmol of the given product min^{-1} (mg of protein)$^{-1}$.

[d] ND, not detected.

[e] $\tilde{R}_{Bz} = V_{PAC}/V_{AL}$ under given conditions.

reaction with 2-ketobutyrate, its concentration drops rapidly before sufficient PAC has been formed for accurate analysis. However, the results at higher 2-ketobutyrate concentrations (Fig. 4) show clearly that PAC formation is essentially completely inhibited by the competing substrate 2-ketobutyrate.

Mutation of Trp^{464} to another amino acid leads to an active enzyme with a greatly reduced preference for 2-ketobutyrate as second substrate (9). The influence of replacement of this residue on the ability of the enzyme to form *R*-PAC seems to be totally unrelated to its effect on the specificity of the enzyme toward 2-ketobutyrate. Fig. 5 shows the behavior of mutein W464L. The preference of this mutein for formation of acetohydroxybutyrate (Fig. 5*A*) is 20-fold less than that of the wild-type, whereas its specificity for formation of *R*-PAC (Fig. 5*B*) is

not very different from that of the wild type ($\tilde{R}_{Bz}$ = 0.9). The mutein W464Q shows a similar pattern of competition (Table I).

The effects of replacement of Trp^{464} can be rationalized if its indole ring interacts with the methyl group of 2-ketobutyrate, as we have suggested (9), stabilizing intermediates on the pathway to acetohydroxybutyrate but not to acetolactate. The inverse stereochemistry of the reaction with benzaldehyde (Fig. 2) implies that the aldehydic hydrogen points toward Trp^{464}, so that there would be no significant interactions between benzaldehyde and this side chain in the course of the reaction, and the formation of PAC should be indifferent to mutation of Trp^{464}. In accord with the suggestion that the carboxylate of a ketoacid and the aromatic ring of benzaldehyde must occupy similar regions of the active site, it is significant that ketoacids carrying *both* a carboxylate and a phenyl group, benzoylformate or phenylpyruvate, are neither substrates of AHAS II nor inhibitors of its reactions with pyruvate (data not shown).

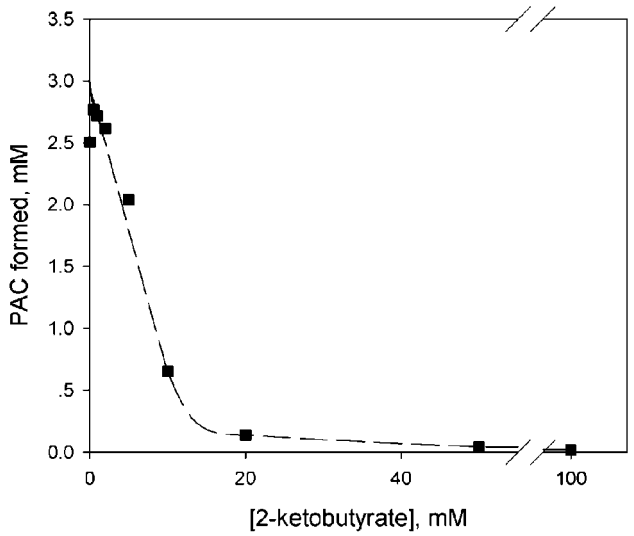

FIG. 4. **Effect of 2-ketobutyrate concentration on the formation of PAC (■) by 100 μg/ml wild-type AHAS II in the presence of 10 mM each of benzaldehyde and pyruvate.** Conditions were otherwise as in Fig. 3, except that the solvent contained 2% Me_2SO. Aliquots after 10 min were analyzed by HPLC. The *line* is an aid to visualization only, since initial rates are inaccurate at the lowest ketobutyrate concentrations (see "Results").

A Model for the Structure of HEThDP⁻ in the site of AHAS II—The recently published structure of the complex of the catalytic subunits of AHAS from the yeast *Saccharomyces cerevisiae* with the sulfonylurea herbicide chlorimuron ethyl (RCSB structural data base entry 1N0H) (11) allows us to place these observations in a structural context and to consider which additional residues in the active site might make contacts with a reacting second ketoacid or benzaldehyde molecule. Fig. 6 shows a tentative structure for the relevant region of the active site of AHAS II, based on the structure of the yeast enzyme-chlorimuron ethyl (CIE) complex. The residues shown are present in most AHASs (including the yeast enzyme and AHAS II), and their structural neighbors are also identical in most AHASs or have conservative replacements. Table II relates the sequence numbering of the relevant residues in AHAS II and yeast AHAS. Many other AHASs, including all of the *E. coli* isozymes, the single *Bacillus stearothermophilus* enzyme, and the yeast enzyme, are also capable of catalyzing condensation with benzaldehyde (results not shown).

We attempted to fit a molecule of 2-ketobutyrate into the active site of AHAS II in accord with this structure and with the stereochemistry of the product acetohydroxybutyrate (see Fig. 7*A*). It seemed reasonable from this model that Arg^{276} might be involved in stabilizing the carboxylate of this substrate in the active site, whereas Trp^{464} interacts with the methyl group. Residue Arg^{276} would then be critical for formation of acetohydroxyacid products but would not be expected to affect the reaction with benzaldehyde (see Fig. 10).

Acetolactate and PAC Synthesis in Muteins—In order to test this idea, we prepared several variants of AHAS II, with Arg^{276} substituted by methionine, phenylalanine, glutamine, or lysine. Each of these mutants is seriously impaired in its ability to synthesize acetohydroxyacids (Table I). However, in the

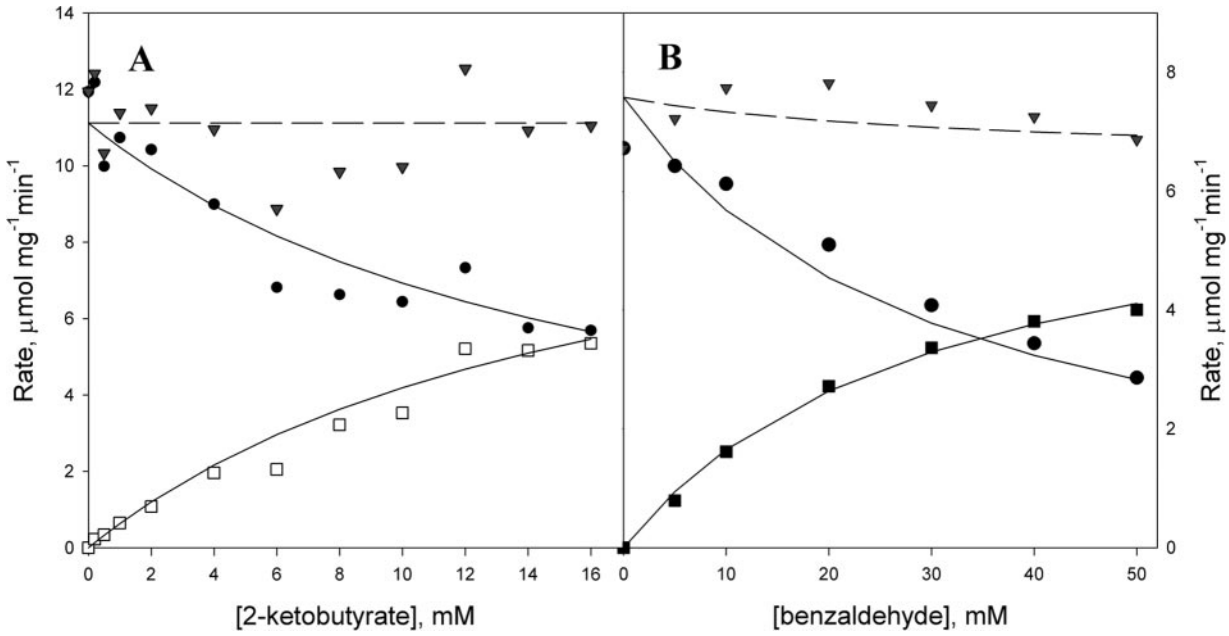

FIG. 5. *A*, effect of 2-ketobutyrate concentration on the initial rates of formation of acetohydroxybutyrate (□) and acetolactate (●), at constant pyruvate concentration (50 mM), with 6 μg/ml His′-AHAS II-W464L. The sum of the rates of formation of the two acetohydroxyacids (▼) is also shown. *B*, effect of benzaldehyde on the initial rates of PAC (■) and acetolactate (●) formation by His′-AHAS II-W464L. The sum of the rates of formation of the two products (▼) is also shown. The reaction was carried out with 200 μg/ml enzyme at 30 °C for 5 min. Other details are as in Fig. 3.

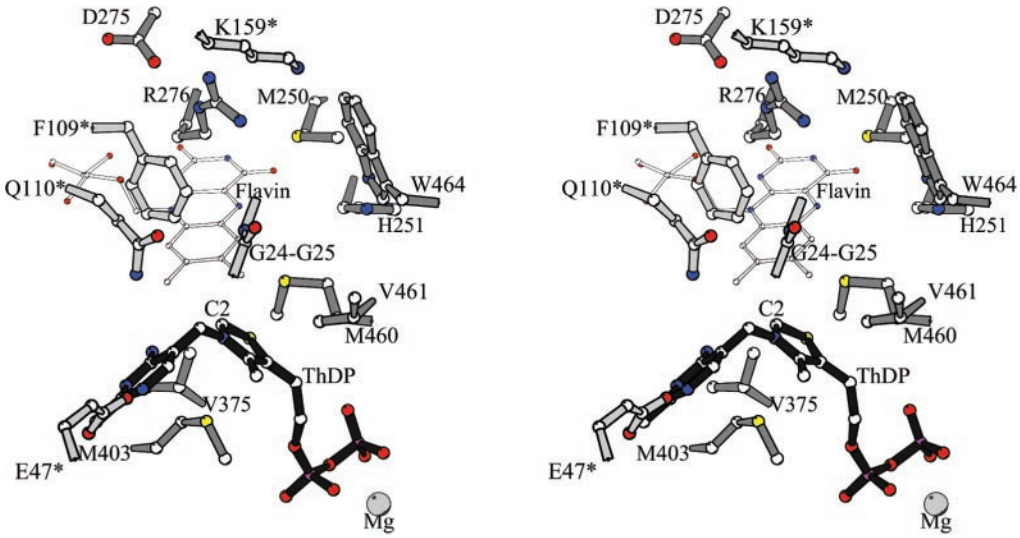

FIG. 6. **Stereo diagram of the active site of AHAS II, based on the structure of the yeast AHAS·CIE complex (Protein Data Bank entry 1NOH) (11).** The residues are labeled with the numbering of AHAS II (see Table II), and residues belonging to the second catalytic polypeptide are marked with an *asterisk*. Thiamin diphosphate is shown with *dark bonds*, with its aminopyrimidine to the left and diphosphate to the right. C-2, the activated carbon, is labeled. The riboflavin moiety of FAD is shown as a *thin white ball-and-stick structure* to avoid confusion in viewing the figure. The program MOLSCRIPT was used to make this figure. Conformation A of Trp^{586} in Protein Data Bank entry 1N0H was used for Trp^{464}.

TABLE II
Relation between sequence numbering of relevant residues in E. coli AHAS II and the S. cerevisiae AHAS

AHAS II	Yeast position
Gly^{25}	116
Phe^{109}	201
Gln^{110}	202
Lys^{159}	251
Met^{250}	354
Arg^{275}	379
Arg^{276}	380
Met^{460}	582
Trp^{464}	586

presence of equimolar concentrations of benzaldehyde and pyruvate, they produce *R*-PAC at 29, 30, 18, and 124%, respectively, of the wild-type rate, and each of them has a preference for formation of *R*-PAC, $\tilde{R}_{Bz}$, more than 10 times that of the wild-type (Table I). In these muteins, the steps involving the acceptor substrates (step 2 and/or 3 in the formation of acetolactate and step 4 and/or 5 in the formation of PAC) (Fig. 1) apparently are rate-determining, since the total rate of acetohydroxyacid synthesis increases with the 2-ketobutyrate concentration (*e.g.* Fig. 8*A*) and the total rate of product formation increases with the benzaldehyde concentration (see Fig. 8*B*). These results provide strong support for the proposal that the positively charged guanidinium group of Arg^{276} is involved in stabilization of the carboxylate of a reacting ketoacid. Lysine can only partially replace the function of arginine; the exact positioning of the positive charge is apparently crucial. From the extrapolated rate of acetohydroxybutyrate formation by mutein R276K at saturation with 2-ketobutyrate (Fig. 8*A*), the rate constant for the conversion of the enzyme-HEThDP$^-$ intermediate to product (Fig. 2, steps 2 and 3) can be estimated to be $\sim$13 s^{-1}, some 2 orders of magnitude lower than the measured rate for the wild-type protein (17).

Muteins R276M, R276Q, and R276F are even more crippled in accepting a ketoacid second substrate (*e.g.* see Fig. 9 and Table I). Their low specificity for formation of acetohydroxybutyrate ($R \leq 1$) indicates that the C-4 methyl of 2-ketobutyrate does not make significant stabilizing contacts with the active site of these muteins at the transition state(s) for product formation, despite the presence of Trp^{464}. This suggests that the reacting second ketoacid might make entirely different contacts with the active site in these muteins and raises the possibility that the stereochemistry of the product of these crippled enzymes might be different. However, when we followed the progress of the reactions of the enzymes modified at Arg^{276} by circular dichroism, we found that they also produce *S*-acetolactate with high enantiomeric specificity (not shown).

The specific activity of the mutein M250A in the synthesis of acetolactate, in the presence of pyruvate as sole substrate, is 1 order of magnitude lower than that of the wild-type. It is almost as active as the wild-type enzyme, however, in the synthesis of PAC (Table I). The catalytic properties of this mutein are thus rather similar to those of the R276K mutein. The side chain of Met^{250} lies between those of Trp^{464} and Arg^{276} and makes close contacts with them. One reasonable explanation for the behavior of the M250A mutein might be that its replacement affects the critical conformation of the positively charged side chain of Arg^{276}.

The aromatic ring of Phe^{109} is also in contact with Arg^{276} (note that these two neighboring side chains come from two different catalytic subunits). When Phe^{109} was mutated to an amino acid with a smaller (Leu) or more flexible (Met) nonpolar side chain, the enzyme lost most of its activity as an acetolactate synthase. However, it retained high activity in the synthesis of PAC (Table I). Mutein F109W has very low activity in both synthetic reactions; the large side chain of a Trp residue at this position apparently interferes with any incoming substrate.

DISCUSSION

Our understanding of the mechanism by which AHAS recognizes its substrates and catalyzes the formation of a specific new carbon-carbon bond has been hampered by the lack of good experimental tools for studying the effects of modifications of the enzyme on the final, product-determining steps of the reaction. The recently discovered ability of AHASs to catalyze the condensation of benzaldehyde with the "active acetaldehyde" moiety derived from pyruvate to form PAC (18) provides such a tool. At saturation with benzaldehyde, wild-type enzyme catalyzes formation of PAC at a velocity comparable with that of formation of the acetohydroxyacids in its absence. The simultaneous measurement of both reactions is simple and conven-

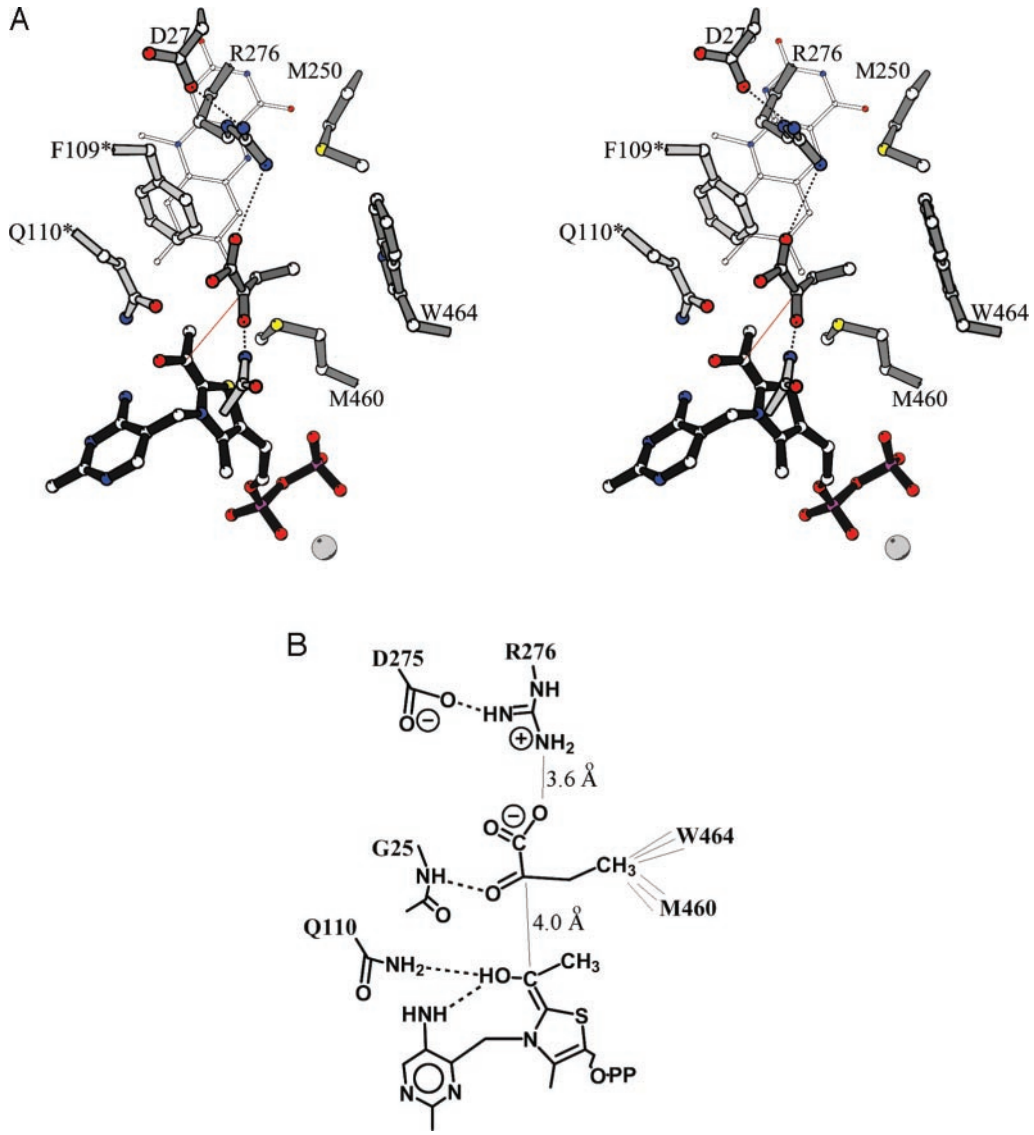

FIG. 7. *A*, stereo picture of the proposed structure for 2-ketobutyrate in the active site of the AHAS II-HEThDP$^-$ intermediate. The angle of view is slightly different from that in Fig. 6, and peripheral residues have been eliminated so that the substrate can be visualized. A *thin dotted red line* connects the nucleophilic carbon of HEThDP$^-$ and the carbonyl carbon of 2-ketobutyrate. Hydrogen bonds of interest are marked with *dashed lines*. *B*, *schematic diagram* with distances.

ient (18). The high stereochemical specificity of the formation of both *S*-acetohydroxyacids and *R*-PAC by AHAS implies that the paths to formation of both kinds of product involve close interactions with the enzyme active site. It is clear that the interactions of 2-ketobutyrate and benzaldehyde with the active site are exclusive, since PAC formation is completely inhibited in the presence of a high concentration of 2-ketobutyrate (Fig. 4).

From the time we constructed our homology model for AHAS II (9), we have been puzzled by the identity of the group or groups in the active site involved in recognition of the carboxylate of the second ketoacid substrate. The structure of the active site predicted in our model was quite similar to the recently published experimental structure, with one important exception; in the yeast AHAS·CIE complex, the guanidinium group of Arg^{380} forms a close interaction with the urea oxygen of the bound sulfonylurea herbicide in the active site (11), whereas in our original homology model the side chain of its homolog in AHAS II, Arg^{276}, pointed in the opposite direction and was far from the active site. Whereas the closer of the two N-η nitrogens of Arg^{380} is 9.5 Å from C-2 of ThDP in the yeast structure, it was 23 Å away in our previous model.

The differential effects of mutagenesis of the four amino acid residues Trp^{464}, Arg^{276}, Met^{250}, and Phe^{109} in AHAS II on the formation of acetolactate, acetohydroxybutyrate, and PAC now allow us to suggest specific functional roles for some of these residues in the product-determining phase of the reaction. Trp^{464} is crucial for the differential recognition of 2-ketobutyrate but apparently does not interact at all with benzaldehyde (Fig. 5 and Table I). Arg^{276} is an important element in the recognition of either of the physiological second 2-ketoacid substrates, so that the formation of acetohydroxyacid products is slowed in muteins altered at this residue, and the product-forming steps (Fig. 1, step 2 and/or 3) become rate-determining (*e.g.* see Fig. 8). On the other hand, Arg^{276} is not important for the reaction with benzaldehyde (Table I).

An hypothetical structure (based on the yeast AHAS·CIE crystal structure (11)) for the AHAS II·HEThDP$^-$ complex with a molecule of 2-ketobutyrate in position to form a new C–C bond is shown in Fig. 7; the carbonyl carbon is about 4 Å from the nucleophilic carbon of HEThDP$^-$. The stereochemistry of the product *S*-acetohydroxybutyrate (25) dictates the relative positions of the carboxylate and ethyl moieties of the reacting ketoacid. The properties of the muteins described above sug-

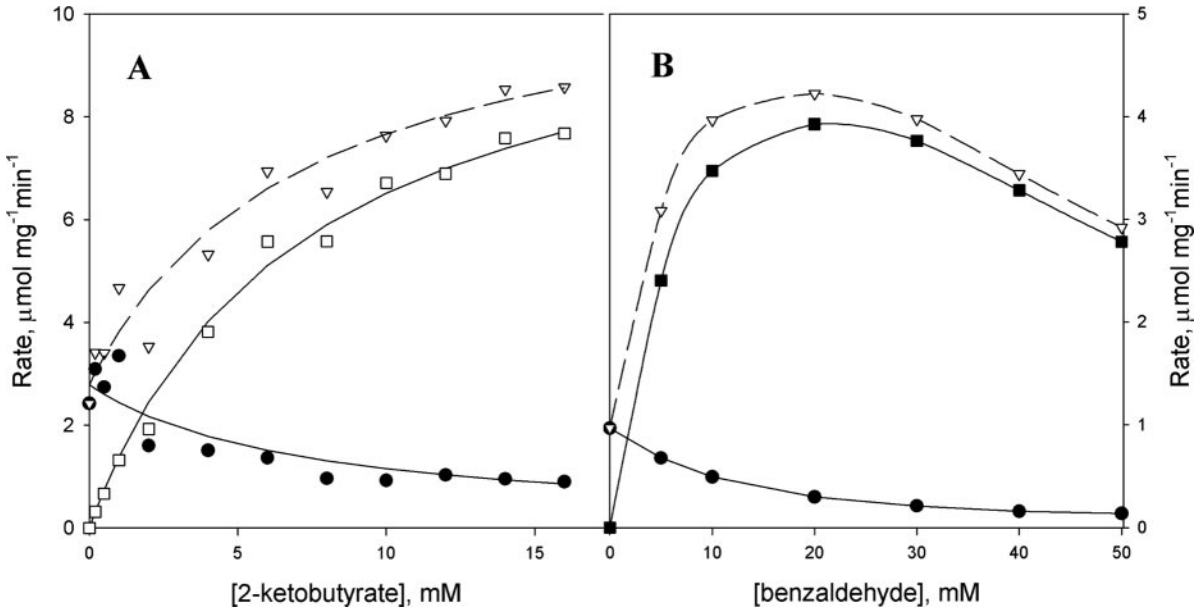

FIG. 8. *A*, effect of 2-ketobutyrate concentration on the initial rates of formation of acetohydroxybutyrate (□) and acetolactate (●), at constant [pyruvate] (50 mM), with 16.8 μg/mg His′-AHAS II-R276K. The sum of the rates of formation of the two acetohydroxyacids (▽) is also shown. *B*, effect of benzaldehyde on the initial rates of PAC (■) and acetolactate (●) formation by His′-AHAS II-R276K. The sum of the rates of formation of the two products (▽) is also shown. The reaction was carried out with 100 μg/ml enzyme at 30 °C for 10 min. Other details are as in Fig. 3.

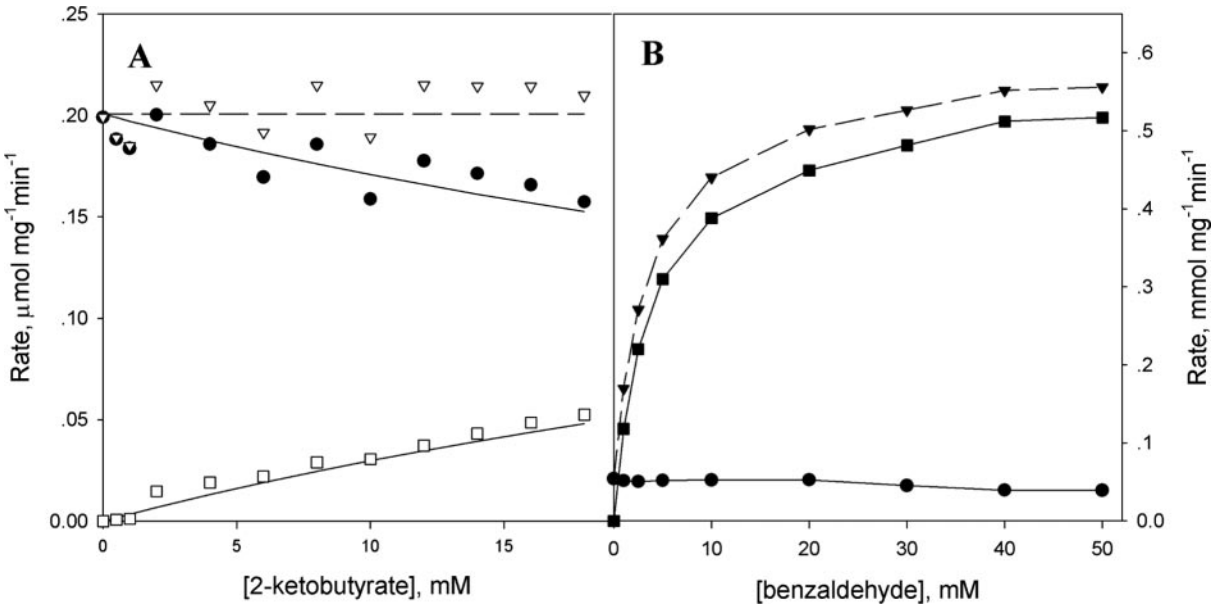

FIG. 9. *A*, effect of 2-ketobutyrate concentration on the initial rates of formation of acetohydroxybutyrate (□) and acetolactate (●), at constant [pyruvate] (50 mM), with 720 μg/mg His′-AHAS II-R276Q. The sum of the rates of formation of the two acetohydroxyacids (▽) is also shown. *B*, effect of benzaldehyde on the initial rates of PAC (■) and acetolactate (●) formation by His′-AHAS II-R276Q. The sum of the rates of formation of the two products (▼) is also shown. The reaction was carried out with 100 μg/ml enzyme at 30 °C for 10 min. Other details are as in Fig. 3.

gest the specific interactions shown in this structure (Fig. 7*B*); one carboxylate oxygen of 2-ketobutyrate points toward a positive η nitrogen of Arg^{276}, and the C4-methyl of the substrate is in van der Waals contact with the aromatic ring of Trp^{464} and perhaps with the side chain of Met^{460}. In this figure, a substrate carboxylate oxygen and an arginine guanidinium nitrogen are 3.6 Å apart, but it is reasonable to assume that movement of the arginine side chain relative to its position in the experimental crystal structure might bring them closer.

Fig. 10 shows a molecule of benzaldehyde in the active site, in a position to form a new C–C bond to $HEThDP^-$. The carbonyl oxygen of benzaldehyde has been placed in a position equivalent to that of the carbonyl of acetohydroxybutyrate in Fig. 7, since we postulate that the protonation of the carbonyl oxygen, as the new C–C bond is being formed, involves the same proton donor in the two reactions (step 2 or step 4 in Fig. 1). The stereochemistry of the product *R*-PAC then dictates the region where the aromatic ring of benzaldehyde must lie. The aromatic ring of benzaldehyde would be too far from Arg^{276} to be influenced by modification of that residue and far from contact with Trp^{464}. Although the aromatic ring might be in van der Waals contact with the side chain of Phe^{109}, the effect of replacement of Phe^{109} on acetolactate formation is much more drastic than its effect on PAC formation.

Mutein R276K has a very high specificity for formation of PAC, $\tilde{R}_{Bz}$, and its k_{cat}/K_m for pyruvate is 40-fold less than that of the wild-type enzyme. In the crystal structure of the yeast enzyme, the arginine side chain homologous to Arg^{276} forms a

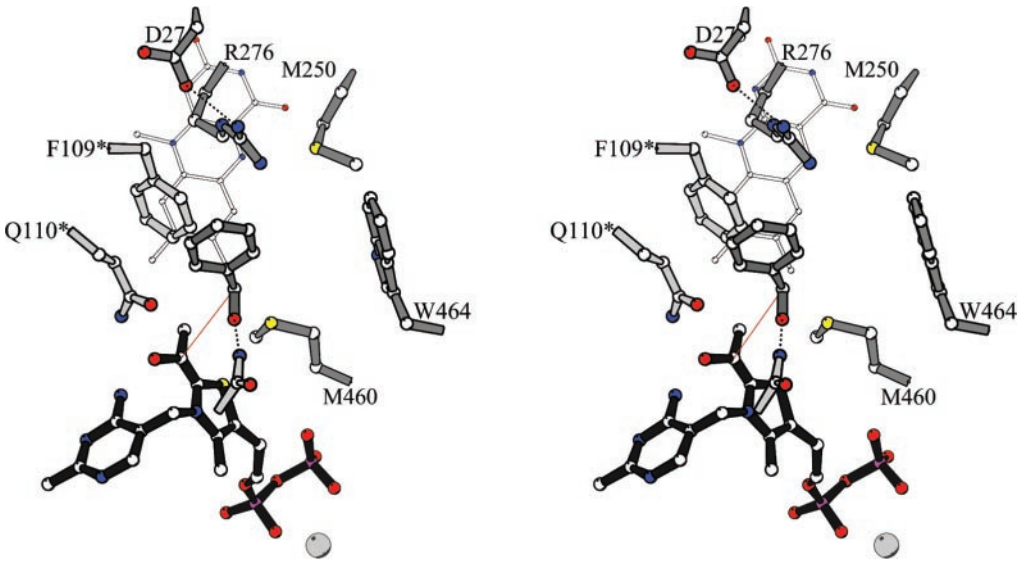

FIG. 10. **Stereo picture of the proposed structure for benzaldehyde in the active site of the AHAS II-HEThDP$^-$ intermediate.** Other details are as in Fig. 7*A*.

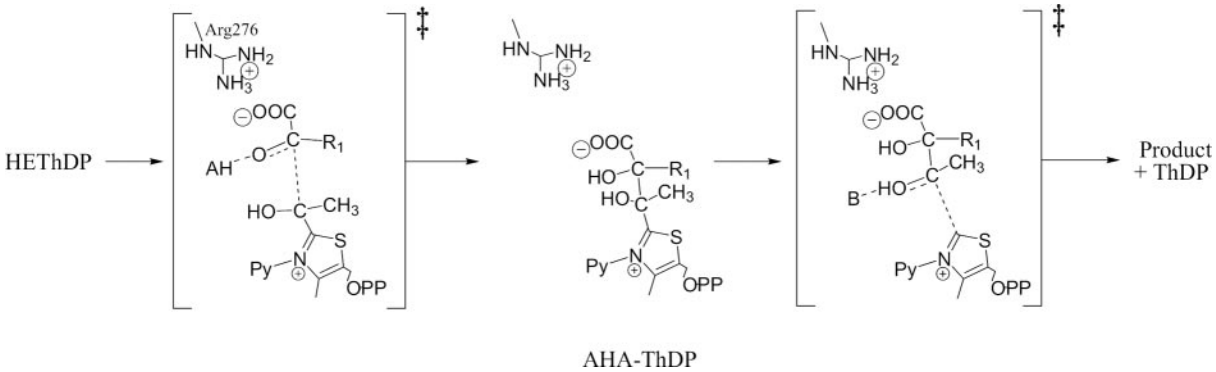

FIG. 11. **Transition states for steps 2 and 3 in the formation of an acetohydroxyacid by AHAS II, with the proposed interaction of the carboxylate with Arg^{276}.**

hydrogen bond with a conserved neighboring aspartate (Fig. 6). It is likely that in mutein R276K the ϵ-amino group of lysine makes a similar hydrogen bond to Asp^{275}, so that the local structure of the active site (and thus full activity in PAC formation) is preserved, but the crucial interaction of the positive charge with the carboxylate of a ketoacid is not possible.

Muteins in which the positive charge of Arg^{276} is completely eliminated are severely crippled in the synthesis of acetolactate and have a low differential specificity for reaction with 2-ketobutyrate in the presence of pyruvate ($R < 1$) (Table I). These properties suggest that a second ketoacid substrate makes different contacts in these muteins than in the wild type. However, the fact that these enzymes form *S*-acetolactate with high enantiomeric specificity indicates that additional factors contribute to the stereochemistry. In particular, reversal of the stereochemistry would place the carboxylate of the incoming pyruvate in a rather hydrophobic environment (*e.g.* near Met^{460}, Trp^{464}, and the dimethylbenzene ring of FAD) (Fig. 7).

It is important to point out that Arg^{276} would be rather far (more than 5 Å) from the acetohydroxyacid carboxylate in the bound covalent product-ThDP complex. However, the interaction between this arginine residue and the carboxylate is likely to be much stronger in the transition states for step 2 and/or 3, in which the C–C bond being made or broken is much longer (Fig. 11). We believe that the effects of mutation of Arg^{276} strongly support a role for this residue in one or both of these steps, as shown schematically in Fig. 11. The contribution of a specific substrate-enzyme interaction to catalysis is expected to be maximized if the interaction is much stronger in the transition state than in the intermediates that precede or follow it (26).

The properties of muteins M250A, F109M, and F109L are reminiscent of those of R276K. These properties can probably also be explained on the basis of the role of the two side chains flanking Arg^{276} in maintaining the conformation of Arg^{276} (Fig. 7). Mutein F109W has low activity in all the reactions tested here; it presumably has too crowded an active site to bind either a ketoacid or benzaldehyde in an appropriate position for rapid nucleophilic attack by HEThDP$^-$.

The oxygenase reaction catalyzed by AHAS II, leading to formation of peracetate from pyruvate, provides another piece of evidence about the reaction of the acceptor substrate (15). The oxygenase activity is inhibited hyperbolically by increasing concentrations of pyruvate or by the addition of ketobutyrate. However, this activity is not completely inhibited, and a finite residual oxygenase activity remains at saturation (15). This implies that the second ketoacid substrate binds reversibly before forming a new bond, in a manner that still allows access by molecular oxygen to the HEThDP$^-$ intermediate. If the reversibly bound second ketoacid is near Arg^{276}, oxygen should be able to attack HEThDP$^-$ in such a complex.

There are, no doubt, other significant contributors to catalysis of product formation in the active site of AHAS. One might consider a role for Gln^{110} in proton transfer to the carbonyl

oxygen of the second substrate. Mutation of this highly conserved residue leads to a significant loss of activity, but it apparently affects the formation of $HEThDP^-$ as well as its conversion to products.[4] The peptide NH of Gly^{25} might also stabilize the incipient negative charge on the carbonyl oxygen as the adduct is formed (Fig. 7).

Lys^{251} (homologous to Lys^{159} in AHAS II) is another residue of yeast AHAS in close contact with the bound sulfonylurea in the enzyme-inhibitor complex (11). Duggleby and co-workers suggest (27), by analogy with the mechanism they propose for the non-FAD-dependent catabolic acetolactate synthase, that Lys^{251} is the important residue for recognition of the carboxylate of the incoming substrate in yeast AHAS. However, this residue is even farther from the reaction site than Arg^{380} (Arg^{276} in AHAS II) and thus less likely to be crucial for catalysis. Mutations at Lys^{251} in the yeast enzyme were identified in the classic sulfonylurea resistance selection experiments carried out by Mazur and Falco (28), but the altered enzymes must have retained sufficient acetohydroxyacid synthase activity to support cell growth and thus be detected. The analogous tobacco AHAS muteins K255Q and K255F are resistant to three classes of herbicides that target AHAS but are reported to have values of k_{cat}/K_m only 5- and 10-fold lower than the wild type (29). It may be significant in this regard that no spontaneous herbicide-resistant mutations at residues homologous to Arg^{276} or Phe^{109} in AHAS II have been reported to date.

Conclusions—The synthesis of *R*-PAC by AHAS, aside from its potential practical use (18), provides a simple but powerful method to examine the recognition of "second substrates" and the specific catalysis of their condensation with $HEThDP^-$. This reaction has allowed us to assign an important role to Arg^{276} in the specificity and reactivity of AHAS II, to confirm the role of Trp^{464}, and to gain new insight into how the enzyme functions. This study also provides a reciprocal benefit; the information it has provided makes it possible to engineer the active site of an AHAS so that it efficiently and preferentially catalyzes a new reaction.

The contribution of additional residues in the active site of AHAS II, such as Lys^{159}, to the catalysis of steps following the formation of $HEThDP^-$ can now be screened using this approach. The details of the kinetics of some of the most interesting muteins (*e.g.* those mutated at Arg^{276}) unveiled in this way will be further examined. In particular, it will be interesting to see whether step 2, step 3, or both steps in the reaction (Fig. 1) are affected by replacement of Arg^{276}. The rapid mixing-quench NMR method (17) should allow us to address this point.

Other interesting questions remain to be answered using the alternative substrate approach. It can be used to follow the reversal of steps 2 and 3 in the formation of acetolactate (Fig. 1) and thus to further map out the energetics of AHAS catalysis. The detailed contribution of residues in the active site of other AHASs (*e.g.* AHAS I) may be quite different than in AHAS II. The influence of electronic effects on the reaction can be probed using substituted benzaldehydes as substrates, and the steric constraints imposed by the active site can be explored over a wide range of substrates with relatively reactive carbonyl groups.

[4] M. Vyazmensky, unpublished results.

REFERENCES

1. Green, J. B. (1989) *FEBS Lett.* **246,** 1–5
2. Bowen, T. L., Union, J., Tumbula, D. L., and Whitman, W. B. (1997) *Gene (Amst.)* **188,** 77–84
3. Chang, Y.-Y., and Cronan, J. E., Jr. (1988) *J. Bacteriol.* **170,** 3937–3945
4. Muller, Y. A., Schumacher, G., Rudolph, R., and Schulz, G. E. (1994) *J. Mol. Biol.* **237,** 315–335
5. Dobritzsch, D., Konig, S., Schneider, G., and Lu, G. (1998) *J. Biol. Chem.* **273,** 20196–20204
6. Arjunan, P., Umland, T., Dyda, F., Swaminathan, S., Furey, W., Sax, M., Farrenkopf, B., Gao, Y., Zhang, D., and Jordan, F. (1996) *J. Mol. Biol.* **256,** 590–600
7. Huebner, G., Tittmann, K., Killenberg-Jabs, M., Schaeffner, J., Spinka, M., Neef, H., Kern, D., Kern, G., Schneider, G., Wikner, C., and Ghisla, S. (1998) *Biochim. Biophys. Acta* **1385,** 221–228
8. Bar-Ilan, A., Balan, V., Tittmann, K., Golbik, R., Vyazmensky, M., Hubner, G., Barak, Z., and Chipman, D. M. (2001) *Biochemistry* **40,** 11946–11954
9. Ibdah, M., Bar-Ilan, A., Livnah, O., Schloss, J. V., Barak, Z., and Chipman, D. M. (1996) *Biochemistry* **35,** 16282–16291
10. Pang, S. S., Duggleby, R. G., and Guddat, L. W. (2002) *J. Mol. Biol.* **317,** 249–262
11. Pang, S. S., Guddat, L. W., and Duggleby, R. G. (2003) *J. Biol. Chem.* **278,** 7639–7644
12. Ciskanik, L. M., and Schloss, J. V. (1985) *Biochemistry* **24,** 3357
13. Barak, Z., Chipman, D. M., and Gollop, N. (1987) *J. Bacteriol.* **169,** 3750–3756
14. Gollop, N., Damri, B., Barak, Z., and Chipman, D. M. (1989) *Biochemistry* **28,** 6310–6317
15. Tse, J. M. T., and Schloss, J. V. (1993) *Biochemistry* **32,** 10398–10403
16. Schloss, J. V., Hixon, M. S., Chu, F., Chang, S., and Duggleby, R. G. (1996) in *Biochemistry and Physiology of Thiamin Diphosphate Enzymes* (Bisswanger, H., and Schellenberger, A., eds) pp. 580–585, A. u. C. Intemann, Wissenschaftlicher Verlag, Prien, Germany
17. Tittmann, K., Golbik, R., Uhlemann, K., Khailova, L., Schneider, G., Patel, M., Jordan, F., Chipman, D. M., Duggleby, R. G., and Hubner, G. (2003) *Biochemistry* **42,** 7885–7891
18. Engel, S., Vyazmensky, M., Geresh, S., Barak, Z., and Chipman, D. M. (2003) *Biotechnol. Bioeng.* **84,** 833–840
19. Krampitz, L. O. (1948) *Arch. Biochem.* **17,** 81–85
20. Aulabaugh, A., and Schloss, J. V. (1990) *Biochemistry* **29,** 2824–2830
21. Crout, D. H. G., McIntyre, C. R., and Alcock, N. W. (1991) *J. Chem. Soc. Perkin Trans.* **2,** 53–62
22. Hill, C. M., Pang, S. S., and Duggleby, R. G. (1997) *Biochem. J.* **327,** 891–898
23. Ho, S. N., Hunt, H. D., Horton, R. M., Pullen, J. K., and Pease, L. R. (1989) *Gene (Amst.)* **77,** 51–59
24. Chipman, D., Barak, Z., and Schloss, J. V. (1998) *Biochim. Biophys. Acta* **1385,** 401–419
25. Crout, D. H. G., Lee, E. R., and Rathbone, D. L. (1990) *J. Chem. Soc. Perkin Trans.* **1,** 1367–1370
26. Leatherbarrow, R. J., Fersht, A. R., and Winter, G. (1985) *Proc. Natl. Acad. Sci. U. S. A.* **82,** 7840–7844
27. Pang, S. S., Duggleby, R. G., Schowen, R. L., and Guddat, L. W. (2004) *J. Biol. Chem.* **279,** 2242–2253
28. Mazur, B., and Falco, S. C. (1989) *Annu. Rev. Plant Physiol.* **40,** 441–470
29. Yoon, T. Y., Chung, S. M., Chang, S. I., Yoon, M. Y., Hahn, T. R., and Choi, J. D. (2002) *Biochem. Biophys. Res. Commun.* **293,** 433–439